ARCHITECTURE CIVIL ENGINEERING ENVIRONMENT
The Silesian University of Technology No. 1/2011

AN IMPROVED THIN-WALLED SHEAR BEAM STATICS AND STABILITY WITH THE CROSS-SECTION DISTORTION

Ryszard WALENTYŃSKI [a], Robert CYBULSKI [b]

[a] Associate Prof.; Faculty of Civil Engineering, The Silesian University of Technology, Akademicka 5, 44-100 Gliwice, Poland
E-mail address: *Ryszard.Walentyński@polsl.pl*

[b] MSc Eng., PhD student; Faculty of Civil Engineering, The Silesian University of Technology, Akademicka 5, 44-100 Gliwice, Poland
E-mail address: *Robert.Cybulski@polsl.pl*

Received: 15.12.2010; Revised: 02.02.2011, Accepted: 15.03.2011

Abstract

This paper deals with the thin-walled shear beam statics and stability with cross-section distortion. The linear statics based on [10] includes the bending in the cross-section of each wall as a Bernoulli beam, Timoshenko beam behavior (in-plane stretch, bending and shear of walls) with free torsion as a Saint-Venant torsion of the walls in the thin-walled beam's element direction. The material is elastic. The stability phenomenon includes formulation of the element stiffness matrix and the geometry matrix under constant compression load. Then the stiffness matrix and the geometry matrix on the system level with eigenvalue problem formulation are presented.
The purposes of this work are the following: to present the solution of homogeneous differential equations in terms of polynomial solution and solution consisting of the exponential modes on arbitrary chosen thin-walled beam cross-section, to extend theory in reference [10] by the buckling theory, to implement above theories into *MatLab* [14] and create the program which can handle different cases of the thin-walled beam's buckling modes, to compare results given in the program with the existing theories.

Streszczenie

W artykule omówiono zagadnienie statyki i stateczności dla belek cienkościennych z uwzględnieniem dystorsji w jej przekroju. Zagadnienie statyki liniowej opiera się na [10] i uwzględnia zginanie poprzeczne ścian przekroju jako belki Bernoulliego, rozciąganie, zginanie i ścinanie w płaszczyźnie ścian przekroju za pomocą belki Timoshenki wraz ze swobodnym skręcaniem (na podstawie teorii Saint-Venanta) tych ścian dla kierunku podłużnego belki cienkościennej. Rozpatrywany materiał jest sprężysty. Opis stateczności tych belek zawiera zdefiniowanie macierzy sztywności i macierzy geometrycznej dla stałego obciążenia ściskającego.
Głównymi celami tego artykułu jest przedstawienie rozwiązania wielomianowego oraz wykładniczego dla jednorodnych równań różniczkowych dla dowolnie wybranego przekroju belki cienkościennej, rozszerzenie teorii zaprezentowanej w [10] o zagadnienia stateczności (wyboczenia belki cienkościennej), zaimplementowanie omawianej teorii w programie *MatLab* [14] i stworzenie własnego programu *TWBSaS* dla celów porównawczych z innymi istniejącymi teoriami omawiającymi konstrukcje cienkościenne.

Keywords: **Thin-walled; Distortion; Statics; Stability; Bernoulli; Timoshenko.**

1. INTRODUCTION

In this paper analysis of thin-walled beams is presented. Structures in which one dimension is much smaller than others are taken into account. In the classic elastic thin-walled beams theory presented in [4] and [13], the cross-section distortion is neglected. It means that cross-sections of the thin-walled beams maintain their shapes. This assumption gives a serious compu-

tational limitation for modern structures e.g. cold-formed steel profiles, purlins, roof sheets, bridge box girders, regular bridge girders and plate girders.

The design process of thin-walled beams with distortion phenomenon uses plates and shells theories involving large numbers of degrees of freedom. This method is very time consuming for numerical analysis based on the finite element method due to amount of degrees of freedom.

This paper will give a starting point to the development of a new method for analysis of elastic thin-walled beam statics and stability with cross-section distortion. The basis of distortion phenomenon is also well described in [1] and [5]. Proposed method is based on the well known beams theories and finite beams elements enable to model both open and closed thin-walled cross-sections with very few degrees of freedom. For numerical analysis, based on finite element method, program called "Thin-walled beam statics and stability" (*TWBSaS*) [2] was implemented in *MatLab* [14]. Firstly, the cross-section of walls elements are described as Bernoulli beams with no-stretch condition. Secondly, Timoshenko beam behavior such as in-plane stretch, bending and shear of cross-section walls with St. Venant torsion in longitudinal direction of thin-walled beam is presented. Then, thin-walled homogeneous differential equations with their solutions are described with example. Both, beam stiffness matrix and beam geometry matrix formulations are presented. These matrices are used for computation of the stability modes eigenvalues. The proposed theory contains numerical examples with solutions compared with solutions based on the existing thin-walled beams theories [6], [7], [8], [9].

2. LINEAR STATICS OF A THIN-WALLED SHEAR BEAM

Let's consider a linear elastic thin-walled beam (TWB) with prismatic cross-section in a three dimensional space.

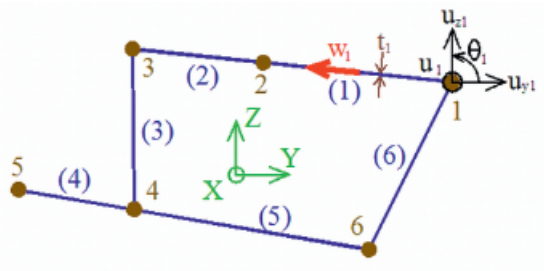

Figure 1.
TWB prismatic cross-section

Fig. 1 presents an example of the TWB cross-section with the sign conventions corresponding to the coordinate system x,y,z. x-axis is defined parallel to the TWB's generator, while y,z-axis describe the plane of the cross-section.

The plane walls (1), (2)…(n_e) (seen as a straight line in the cross-section) between nodes 1,2…n_n have the thickness t_e.

The displacements and the rotation of node n are defined as follows: in x-direction (axial displacement) as u_n, in y,z-directions (cross-section displacements) as u_{yn} and u_{zn}, rotation as θ_n. The in-plane deflection for the wall e is defined by w_e.

From the above components, the cross-sections vectors including all nodes and all walls are as follows: the axial displacement vector **U**, the cross-section displacements vector $\mathbf{V^b}$, the cross-section plane rotation vector $\boldsymbol{\theta}^{\mathbf{b}}$, the in-plane deflections vector **W**.

$$\mathbf{U} = \begin{bmatrix} \cdot \\ u_n \\ \cdot \end{bmatrix}, \mathbf{V^b} = \begin{bmatrix} \cdot \\ u_{yn} \\ u_{zn} \\ \cdot \end{bmatrix}, \boldsymbol{\theta}^{\mathbf{b}} = \begin{bmatrix} \cdot \\ \theta_n \\ \cdot \end{bmatrix}, \mathbf{W} = \begin{bmatrix} \cdot \\ w_e \\ \cdot \end{bmatrix} \quad (1)$$

2.1. Strain energy

The thin-walled shear beam statics with cross-section distortion is briefly described based on [10]. Firstly, bending in the cross-section is presented, secondly, Timoshenko beam behavior with St. Venant torsion of the walls in the TWB direction.

The cross-section bending is considered for each wall as a Bernoulli beam (with wall nodes 1 and 2 connected to cross-section nodes i and j) of length l (see Fig. 2) which cannot change with the displacement.

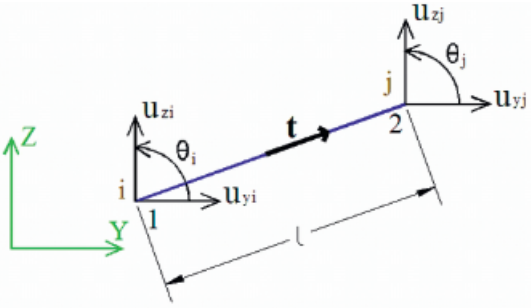

Figure 2.
Arbitrary Burnoulli beam

Vector **t** is a unit vector in the wall direction.

Due to beam length l which cannot change with the

displacement the no-stretch condition for a single wall is presented:

$$\left(u_{yj}-u_{yi},u_{zj}-u_{zi}\right)\cdot\mathbf{t}=0 \tag{2}$$

And for all walls of the cross-section the following is given:

$$\mathbf{A}\mathbf{V}^{b}=0 \tag{3}$$

where matrix **A** of the size $n_e x(2n_n)$ is built up by components from the wall unit vector **t**. Full pivoting factorization of **A** gives the relation between dependent $\mathbf{V}^{bd}$ and independent $\mathbf{V}^{bi}$ cross-section displacements, where $\mathbf{T}^{b}_{vdi}$ is the transformation matrix determined from **A**.

$$\mathbf{V}^{bd}=\mathbf{T}^{b}_{vdi}\mathbf{V}^{bi} \tag{4}$$

The relation between the cross-section displacements $\mathbf{V}^{b}$ and the independent cross-section displacements $\mathbf{V}^{bi}$ is given as follows:

$$\mathbf{V}^{b}=\begin{bmatrix}\mathbf{V}^{bd}\\ \mathbf{V}^{bi}\end{bmatrix}=\begin{bmatrix}\mathbf{T}^{b}_{vdi}\mathbf{V}^{bi}\\ \mathbf{V}^{bi}\end{bmatrix}=\begin{bmatrix}\mathbf{T}^{b}_{vdi}\\ \mathbf{I}\end{bmatrix}\mathbf{V}^{bi}\equiv\mathbf{T}^{b}_{vi}\mathbf{V}^{bi} \tag{5}$$

where last equal sign defines the transformation matrix $\mathbf{T}^{b}_{vi}$.

Now, the relation between the in-plane deflections **W** and the independent cross-section displacements is introduced. For a single wall the relation is presented:

$$w=\left(u_{yi},u_{zi}\right)\cdot\mathbf{t} \tag{6}$$

where only one node of each wall is considered. For all walls of the cross-section the following is given:

$$\mathbf{W}=\mathbf{B}\mathbf{V}^{b} \tag{7}$$

Matrix **B** of the size $n_e x(2n_n)$ is built up by components from the wall unit vector **t**. Inserting Eqn (5) in to Eqn (7) gives the relation:

$$\mathbf{W}=\mathbf{B}\mathbf{T}^{b}_{vi}\mathbf{V}^{bi}\equiv\mathbf{T}^{b}_{wi}\mathbf{V}^{bi} \tag{8}$$

where last equal sign defines the transformation matrix $\mathbf{T}^{b}_{wi}$.

The strain energy W^{b}_{cs} in bending of the cross-section per axial unit length with the summation over the walls is following:

$$W^{b}_{cs}=\frac{1}{2}\sum_{e}\mathbf{v}^{bT}_{e}\mathbf{k}^{b}_{e}\mathbf{v}^{b}_{e} \tag{9}$$

where $\mathbf{k}^{b}_{e}$ is the symmetric wall stiffness matrix for a Bernoulli beam element with axial stiffness $EA^{b}=0$ and bending stiffness. $\mathbf{V}^{b}_{e}$ is the wall DOF vector on the cross-section level.

The strain energy for all walls of the TWB cross-section is determined as follows:

$$W^{b}_{cs}=\frac{1}{2}\begin{bmatrix}\mathbf{V}^{bT} & \boldsymbol{\theta}^{bT}\end{bmatrix}\begin{bmatrix}\mathbf{K}^{b}_{vv} & \mathbf{K}^{b}_{v\theta}\\ \mathbf{K}^{b}_{\theta v} & \mathbf{K}^{b}_{\theta\theta}\end{bmatrix}\begin{bmatrix}\mathbf{V}^{b}\\ \boldsymbol{\theta}^{b}\end{bmatrix} \tag{10}$$

where $[\mathbf{V}^{bT}\ \boldsymbol{\theta}^{bT}]$ is the cross-section DOF vector and $\mathbf{K}^{b}$ is the stiffness matrix assembled from $\mathbf{k}^{b}_{e}$.

$$\mathbf{K}^{b}=\begin{bmatrix}\mathbf{K}^{b}_{vv} & \mathbf{K}^{b}_{v\theta}\\ \mathbf{K}^{b}_{\theta v} & \mathbf{K}^{b}_{\theta\theta}\end{bmatrix} \tag{11}$$

Inserting Eqn(5) into Eqn(10) leads to:

$$W^{b}_{cs}=\frac{1}{2}\begin{bmatrix}\mathbf{V}^{biT} & \boldsymbol{\theta}^{bT}\end{bmatrix}\begin{bmatrix}\mathbf{K}^{b}_{ii} & \mathbf{K}^{b}_{i\theta}\\ \mathbf{K}^{b}_{\theta i} & \mathbf{K}^{b}_{\theta\theta}\end{bmatrix}\begin{bmatrix}\mathbf{V}^{bi}\\ \boldsymbol{\theta}^{b}\end{bmatrix} \tag{12}$$

where last equal sign defines $\mathbf{K}^{b}_{ii}$, $\mathbf{K}^{b}_{i\theta}$, $\mathbf{K}^{b}_{\theta i}$, $\mathbf{K}^{b}_{\theta\theta}$.

Now, let us consider the Timoshenko beam behavior. The strain energy W^{p} per axial unit length in the single wall plane is given as:

$$W^{p}=\frac{1}{2}EA^{p}u^{2}_{,x}+\frac{1}{2}EI^{p}\alpha^{2}_{,x}+\frac{1}{2}GA^{p}_{s}\gamma^{2} \tag{13}$$

with the following displacement field:

$$u=\frac{1}{2}\left(u_i+u_j\right),\alpha=\frac{u_j-u_i}{l},\gamma=\frac{u_j-u_i}{l}+w_{,x} \tag{14}$$

where EA^{p} is the axial stiffness, EI^{p} the bending stiffness, GA^{p}_{s} the shear stiffness, $u_{,x}$ the relative stretch, α the in-plane rotation of the wall's cross-section, γ the angle change in the wall plane. The strain energy for all walls in the cross-section in terms of independent quantities is written as follows:

$$\mathbf{W}^{p}_{cs}=\frac{1}{2}\mathbf{U}^{T}_{,x}\mathbf{D}_{uxux}\mathbf{U}_{,x}+\frac{1}{2}\mathbf{U}^{T}\mathbf{D}_{uu}\mathbf{U}+\frac{1}{2}\mathbf{V}^{biT}_{,x}\mathbf{D}^{p}_{vixvix}\mathbf{V}^{bi}_{,x}+\mathbf{V}^{biT}_{,x}\mathbf{D}_{vixu}\mathbf{U} \tag{15}$$

where matrices $\mathbf{D}_{uxux}$, $\mathbf{D}_{uu}$, D^{p}_{vixvix}, D_{vixu} are the material stiffness matrices.

Last term of the total strain energy corresponds to the St. Venant torsion. The strain energy W^{t} per axial unit length for free torsion about x-direction of a single wall is given as:

$$W^{t}=\frac{1}{2}GI_{t}\tilde{\theta}^{2}_{,x} \tag{16}$$

with the following displacement field:

$$\tilde{\theta}=\frac{1}{l}\left(\left(u_{yj},u_{zj}\right)\cdot\hat{\mathbf{t}}-\left(u_{yi},u_{zi}\right)\cdot\hat{\mathbf{t}}\right),\hat{\mathbf{t}}=\left(-t_z,t_y\right) \tag{17}$$

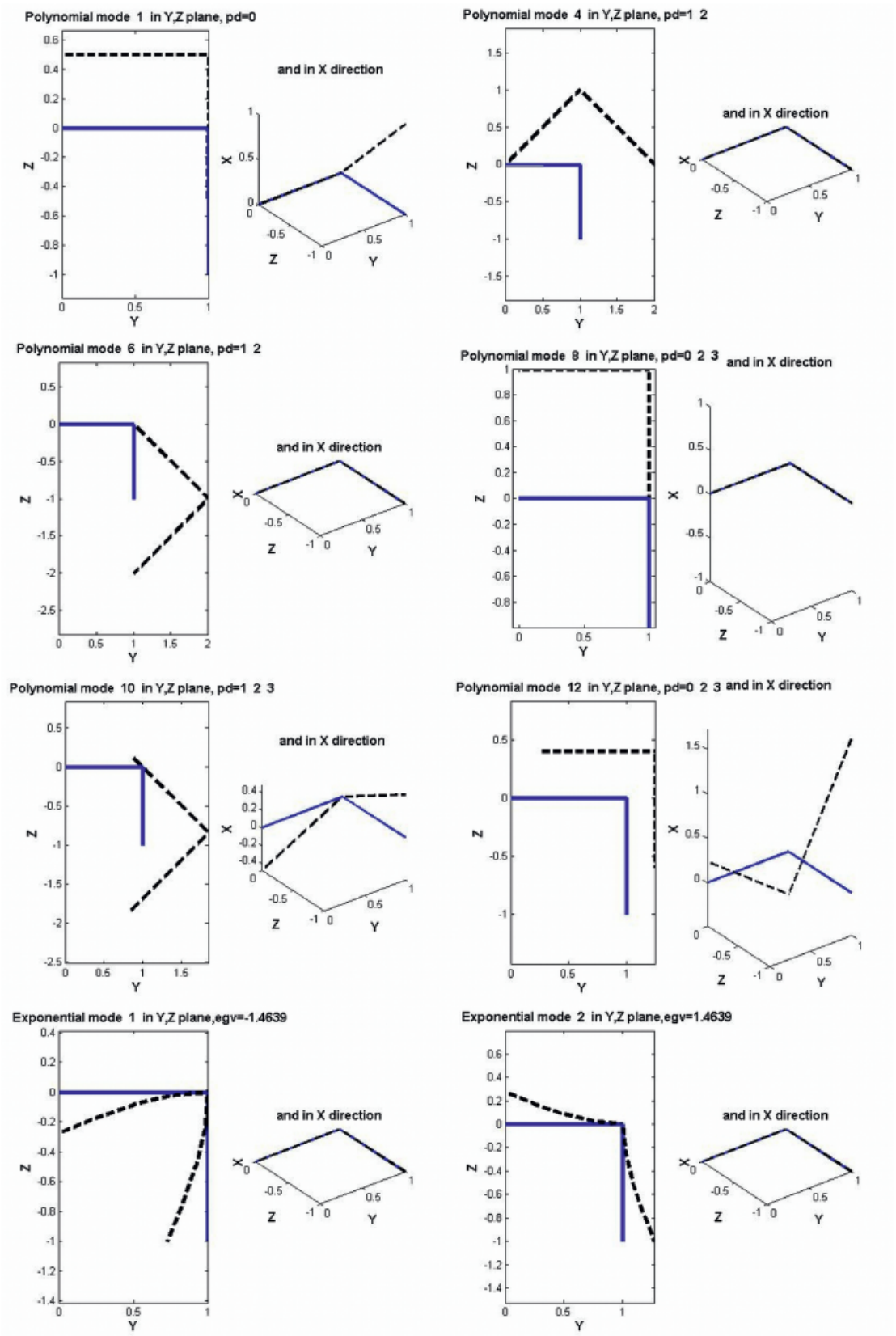

Figure 3.
Polynomial and exponential modes

where GI_t is the torsion stiffness and $\tilde{\theta}$ the rotation in the cross-section plane. The strain energy for all walls in the cross-section in terms of independent quantities is following:

$$W_{cs}^{t} = \frac{1}{2}\mathbf{V}_{,x}^{biT}\mathbf{D}_{vixvix}^{t}\mathbf{V}_{,x}^{bi} \tag{18}$$

where matrix $\mathbf{D}_{vixvix}^{t}$ is the material stiffness matrix.

The total strain energy W_{cs} per axial unit length for the full cross-section is set up from Eqs (12), (15) and (18).

$$W_{cs} = W_{cs}^{b} + W_{cs}^{p} + W_{cs}^{t} \tag{19}$$

Strain energy formulation is well described in [3].

2.2. Solution to the homogeneous differential equations

In this part the homogeneous differential equations derivation with thiers solutions are briefly discussed. From Eqn (19) the virtual work formulation is determined:

$$\begin{aligned}\delta W_{cs} = 0 = [\delta\mathbf{V}^{biT} \quad \delta\boldsymbol{\theta}^{bT}]\begin{bmatrix}\mathbf{K}_{ii}^{b} & \mathbf{K}_{i\theta}^{b}\\ \mathbf{K}_{\theta i}^{b} & \mathbf{K}_{\theta\theta}^{b}\end{bmatrix}\begin{bmatrix}\mathbf{V}^{bi}\\ \boldsymbol{\theta}^{b}\end{bmatrix}\\ + \delta\mathbf{U}_{,x}^{T}\mathbf{D}_{uxux}\mathbf{U}_{,x} +\\ +\delta\mathbf{U}^{T}\mathbf{D}_{uu}\mathbf{U} + \delta\mathbf{V}_{,x}^{biT}\mathbf{D}_{vixvix}\mathbf{V}_{,x}^{bi} + \delta\mathbf{V}_{,x}^{biT}\mathbf{D}_{vixu}\mathbf{U}\\ + \delta\mathbf{U}^{T}\mathbf{D}_{vixu}^{T}\mathbf{V}_{,x}^{bi}\end{aligned} \tag{20}$$

All terms from Eqn (20) with virtual displacement derivatives are integrated by parts over the TWB from the cross-section x=0 to the cross-section x=L. This operation leads to the homogeneous differential equations (written in matrix notation) for the TWB.

$$\mathbf{D}_2\mathbf{u}(x)_{,xx} + \mathbf{D}_1\mathbf{u}(x)_{,x} + \mathbf{D}_0\mathbf{u}(x) = 0 \tag{21}$$

where

$$\begin{aligned}\mathbf{u}(x) = \begin{bmatrix}\mathbf{U}(x)\\ \mathbf{V}^{bi}(x)\end{bmatrix}, \mathbf{D}_2 = \begin{bmatrix}-\mathbf{D}_{uxux} & \mathbf{0}\\ \mathbf{0} & -\mathbf{D}_{vixvix}\end{bmatrix}\\ \mathbf{D}_1 = \begin{bmatrix}\mathbf{0} & \mathbf{D}_{vixu}^{T}\\ -\mathbf{D}_{vixu} & \mathbf{0}\end{bmatrix}, \mathbf{D}_0 = \begin{bmatrix}\mathbf{D}_{uu} & \mathbf{0}\\ \mathbf{0} & \mathbf{K}_{ii}^{b*}\end{bmatrix}\\ \boldsymbol{\theta}^{b} = -\mathbf{K}_{\theta\theta}^{-b}\mathbf{K}_{\theta i}^{b}\mathbf{V}^{bi}, \mathbf{K}_{ii}^{b*} = \mathbf{K}_{ii}^{b} - \mathbf{K}_{i\theta}^{b}\mathbf{K}_{\theta\theta}^{-b}\mathbf{K}_{\theta i}^{b}\end{aligned} \tag{22}$$

The solution to Eqn (21) given by the independent cross-section DOFs $\mathbf{u}(x)$ is partitioned in a polynomial solution $\mathbf{u}^{p}(x)$ and in a solution consisting of n_{exp} exponential modes.

$$\mathbf{u}(x) = \mathbf{u}^{p}(x) + \sum_{m} b_m\,\mathbf{u}_m e^{\lambda_m x} \tag{23}$$

where b_m is a mode factor, $\mathbf{u}_m$ a constant mode vector and λ_m non-zero mode scale.

Using program which is based on the theory presented above and written in *MatLab* [14], six out of twelve randomly chosen polynomial modes and two exponential modes are presented (see Fig. 3) on the L-shaped cross-section with the following data: E=200 GPa (Young modulus), υ=0.3 (Poisson ratio), t=0.01 m (constant thickness for all walls), G=77 GPa (Shear modulus), A=0.02 m^2 (cross-section area), l=1 m (wall length).

The polynomial modes correspond to in-plane translation and rotation, axial rotation, axial translation and elongation, torsion, constant shear and constant moment. The last two modes correspond to the solution which consists of the exponential modes and deformation of the cross-section is observed.

2.3. Stiffness matrix of an element and a system

The TWB element is a part of the TWB between two cross-sections with distance L in the interval 0≤x≤L. The coordinate system is illustrated in Fig. 4. For numerical reasons TWB element's length L is restricted by:

$$L < \frac{1}{\max\lambda_m} \tag{24}$$

due to integration along element's length for the short wave modes.

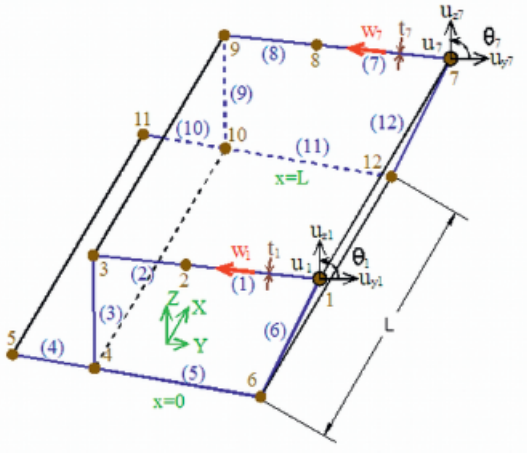

Figure 4.
TWB element

Firstly, the interpolation matrix through the length of the element for polynomial solution must be found. The polynomial solution to Eqn (21) is limited to 3rd degree polynomials:

$$\mathbf{u}^{p}(x)=\begin{bmatrix}u_1^{p}(x)\\ u_2^{p}(x)\\ \vdots\end{bmatrix}=\begin{bmatrix}a_{11} & a_{12} & \cdots\\ a_{21} & a_{22} & \cdots\\ \vdots & \vdots & \vdots\end{bmatrix}\begin{bmatrix}1\\ x\\ x^2\\ x^3\end{bmatrix}\equiv\mathbf{A}\begin{bmatrix}1\\ x\\ x^2\\ x^3\end{bmatrix} \quad (25)$$

where u_i^p is a component of $\mathbf{u}^p$, a_{ij} are unknown constants and last equal sign defines the x-independent coefficient matrix **A**.

Inserting Eqn (25) and its two first derivatives to Eqn (21) and satisfying the solution for all x along TWB leads to:

$$\begin{bmatrix}\mathbf{D}_0 & \mathbf{D}_1 & 2\mathbf{D}_2 & \mathbf{0}\\ \mathbf{0} & \mathbf{D}_0 & 2\mathbf{D}_1 & 6\mathbf{D}_2\\ \mathbf{0} & \mathbf{0} & \mathbf{D}_0 & 3\mathbf{D}_1\\ \mathbf{0} & \mathbf{0} & \mathbf{0} & \mathbf{D}_0\end{bmatrix}\begin{bmatrix}\mathbf{a}_1\\ \mathbf{a}_2\\ \mathbf{a}_3\\ \mathbf{a}_4\end{bmatrix}=\mathbf{0}\Leftrightarrow\mathbf{D}^{a}\mathbf{a}=\mathbf{0} \quad (26)$$

where $\mathbf{a}_j$ is the "jth" column of **A**.

Factorizing $\mathbf{D}^a$ with full pivoting gives a linear relation between a set of independent coefficients $\mathbf{a}^{(i)}$ and a set of dependent coefficients $\mathbf{a}^{(d)}$.

$$\mathbf{a}^{(d)}=\mathbf{T}_{adi}\mathbf{a}^{(i)} \quad (27)$$

The relation between **a** set of coefficients a and a set of independent coefficients $\mathbf{a}^{(i)}$ is given as follows:

$$\mathbf{a}=\begin{bmatrix}\mathbf{a}^{(d)}\\ \mathbf{a}^{(i)}\end{bmatrix}=\begin{bmatrix}\mathbf{T}_{adi}\\ \mathbf{I}\end{bmatrix}\mathbf{a}^{(i)}\equiv\mathbf{T}_{ai}\mathbf{a}^{(i)} \quad (28)$$

where last equal sign defines the transformation matrix $\mathbf{T}_{ai}$.

Now, Eqn (25) becomes:

$$\mathbf{u}^{p}(x)=[\mathbf{a}_1\quad\mathbf{a}_2\quad\mathbf{a}_3\quad\mathbf{a}_4]\begin{bmatrix}1\\ x\\ x^2\\ x^3\end{bmatrix}= \quad (29)$$

$$\begin{bmatrix}\cdot & \cdot & \cdot & \cdot\\ 1 & x & x^2 & x^3\\ \cdot & \cdot & \cdot & \cdot\end{bmatrix}\begin{bmatrix}\mathbf{a}_1\\ \mathbf{a}_2\\ \mathbf{a}_3\\ \mathbf{a}_4\end{bmatrix}$$

$$\equiv\mathbf{N}^{pa}(x)\begin{bmatrix}\mathbf{a}_1\\ \mathbf{a}_2\\ \mathbf{a}_3\\ \mathbf{a}_4\end{bmatrix}$$

where last sign defines the interpolation matrix $\mathbf{N}^{pa}(x)$. Inserting Eqn (28) in Eqn (29) leads to the following polynomial solution:

$$\mathbf{u}^{p}(x)=\mathbf{N}^{pa}(x)\mathbf{a}=\mathbf{N}^{pa}(x)\mathbf{T}_{ai}\mathbf{a}^{(i)}\equiv\mathbf{N}^{p}(x)\mathbf{a}^{(i)} \quad (30)$$

Secondly, the interpolation matrix through the length of the element for exponential solution is investigated. The exponential modes are partitioned in increasing modes m_+ where $Re(\lambda_{m+})>0$ and decreasing modes m_- where $Re(\lambda_{m-})<0$. For numerical reasons the starting point for the increasing modes is taken as x=L and Eqn (23) becomes:

$$\mathbf{u}(x)=\mathbf{N}^{p}(x)\mathbf{a}^{(i)}+\sum_{m_+}b_m\,\mathbf{u}_m e^{\lambda_m(x-L)}+\sum_{m_-}b_m\,\mathbf{u}_m e^{\lambda_m x} \quad (31)$$

Introducing $\mathbf{N}^e$ and **b**

$$\mathbf{N}^{e}(x)=\begin{bmatrix}\cdots & \mathbf{u}_{m_+}e^{\lambda_{m+}(x-L)} & \cdots & \mathbf{u}_{m_-}e^{\lambda_{m-}x}\end{bmatrix}$$
$$\mathbf{b}^{T}=\begin{bmatrix}\cdots & \mathbf{b}_{m_+} & \cdots & \mathbf{b}_{m_-}\end{bmatrix} \quad (32)$$

Eqn (31) takes the following form:

$$\mathbf{u}(x)=[\mathbf{N}^{p}(x)\quad\mathbf{N}^{e}(x)]\begin{bmatrix}\mathbf{a}^{(i)}\\ \mathbf{b}\end{bmatrix}\equiv\mathbf{N}^{\gamma}(x)\boldsymbol{\gamma} \quad (33)$$

where $\mathbf{N}^{\gamma}(x)$ is the interpolation matrix and $\boldsymbol{\gamma}$ the displacement parameter vector. Now the element DOF vector **v** is determined concerning the element end points

$$\mathbf{v}\equiv\begin{bmatrix}\mathbf{u}(0)\\ \mathbf{u}(L)\end{bmatrix}=\begin{bmatrix}\mathbf{N}^{\gamma}(0)\\ \mathbf{N}^{\gamma}(L)\end{bmatrix}\boldsymbol{\gamma}\equiv\mathbf{A}^{\gamma}\boldsymbol{\gamma} \quad (34)$$

where last equal sign defines matrix A^{γ}. Eqn (34) gives $\boldsymbol{\gamma}=(\mathbf{A}^{\gamma})^{-1}\mathbf{v}$ and inserting it to Eqn (33) gives:

$$\mathbf{u}(x)=\mathbf{N}^{\gamma}(x)(\mathbf{A}^{\gamma})^{-1}\mathbf{v}\equiv\mathbf{N}(x)\mathbf{v} \quad (35)$$

where last equal sign defines the interpolation matrix **N**(x).

The interpolation matrix **N**(x) can be presented as follows:

$$\mathbf{N}(x)=\begin{bmatrix}\mathbf{N}^{U}(x)\\ \mathbf{N}^{Vbi}(x)\\ \mathbf{N}^{\theta}(x)\end{bmatrix} \quad (36)$$

$\mathbf{N}^U(x)$ is a part of **N**(x) which is related to the axial displacements and $\mathbf{N}^{Vbi}(x)$ to the independent cross-section displacements. Eqn (36) is extended by the components related to the rotation vector $\boldsymbol{\theta}^b$, denoted as $\mathbf{N}^{\theta}(x)$. This matrix is obtained from Eqn (22).

To compute the element stiffness matrix $\mathbf{k}_{el}$ the strain-displacement matrix **B** has to be found. From the virtual work formulation Eqn (20) the strain vector ε and material stiffness matrix **D** are achieved as follows:

$$\boldsymbol{\varepsilon}^{\mathrm{T}} = \left[\mathbf{U}_{,\mathrm{x}}^{\mathrm{T}} \quad \mathbf{U}^{\mathrm{T}} \quad \mathbf{V}_{,\mathrm{x}}^{\mathrm{biT}} \mathbf{V}^{\mathrm{biT}} \quad \boldsymbol{\theta}^{\mathrm{T}}\right]$$
$$\delta\boldsymbol{\varepsilon}^{\mathrm{T}} = \left[\delta\mathbf{U}_{,\mathrm{x}}^{\mathrm{T}} \quad \delta\mathbf{U}^{\mathrm{T}} \quad \delta\mathbf{V}_{,\mathrm{x}}^{\mathrm{biT}} \delta\mathbf{V}^{\mathrm{biT}} \quad \delta\boldsymbol{\theta}^{\mathrm{T}}\right] \tag{37}$$
$$\mathbf{D} = \begin{bmatrix} \mathbf{D}_{\mathrm{uxux}} & \cdots & \cdots & \cdots & \cdots \\ \cdots & \mathbf{D}_{\mathrm{uu}} & \mathbf{D}_{\mathrm{vixu}}^{\mathrm{T}} & \cdots & \cdots \\ \cdots & \mathbf{D}_{\mathrm{vixu}} & \mathbf{D}_{\mathrm{vixvix}} & \cdots & \cdots \\ \cdots & \cdots & \cdots & \mathbf{K}_{\mathrm{ii}}^{\mathrm{b}} & \mathbf{K}_{\mathrm{i\theta}}^{\mathrm{b}} \\ \cdots & \cdots & \cdots & \mathbf{K}_{\mathrm{\theta i}}^{\mathrm{b}} & \mathbf{K}_{\mathrm{\theta\theta}}^{\mathrm{b}} \end{bmatrix}$$

with 0 entries empty.

Now, the strain-displacement matrix **B** becomes:

$$\mathbf{B}(\mathrm{x}) = \begin{bmatrix} \mathbf{N}_{,\mathrm{x}}^{\mathrm{U}}(\mathrm{x}) \\ \mathbf{N}^{\mathrm{U}}(\mathrm{x}) \\ \mathbf{N}_{,\mathrm{x}}^{\mathrm{V^{bi}}}(\mathrm{x}) \\ \mathbf{N}^{\mathrm{V^{bi}}}(\mathrm{x}) \\ \mathbf{N}^{\theta}(\mathrm{x}) \end{bmatrix} \tag{38}$$

The internal virtual work of TWB element is as follows:

$$\delta \mathrm{W}^{i} = \delta\mathbf{v}^{\mathrm{T}} \left(\int_{0}^{\mathrm{L}} \mathbf{B}^{\mathrm{T}} \mathbf{D} \mathbf{B} \, \mathrm{dx} \right) \mathbf{v} \tag{39}$$

and the element stiffness matrix $\mathbf{k_{el}}$ is defined by:

$$\mathbf{k_{el}} = \int_{0}^{\mathrm{L}} \mathbf{B}^{\mathrm{T}} \mathbf{D} \mathbf{B} \, \mathrm{dx} \tag{40}$$

For TWB which consists of several elements in x direction, the system stiffness matrix is denoted by **K**.

3. FEM FORMULATION FOR STABILITY PROBLEMS

In an in-plane loaded TWB two kinds of displacements can occur: in-plane deflection and deflection perpendicular to the plate plane. These deflections occur when the in-plane load becomes sufficiently large. This is called a stability phenomenon. To present TWB buckling problem the geometry matrix (in [9] called stress-stabilization matrix) must be found, then the eigenvalue problem can be solved. FEM formulation for stability problems is based on [2].

3.1. Geometry matrix of an element and a system

At this stage of research, the TWB element geometry matrix is found for the simple case of constant compression load.

Let's first consider the deflections perpendicular to the plate plane (see Fig. 5). On the cross-section level, one wall consists of DOF vector $\mathbf{v}_{\mathrm{b}}$ and two nodal deflections w_{Li} and w_{Lj}:

$$\mathbf{v}_{\mathrm{b}}^{\mathrm{T}} = [u_{yi}\, u_{zi}\, u_{yj}\, u_{zj}] \tag{41}$$

$$\begin{aligned} w_{Li} &= (u_{yi,} u_{zi}) \cdot \hat{\mathbf{t}} \\ w_{Lj} &= (u_{yj,} u_{zj}) \cdot \hat{\mathbf{t}} \end{aligned} \tag{42}$$

where $\hat{\mathbf{t}}$ is a direction vector defined as

$$\hat{\mathbf{t}} = (t_{z,} - t_{y}) \tag{43}$$

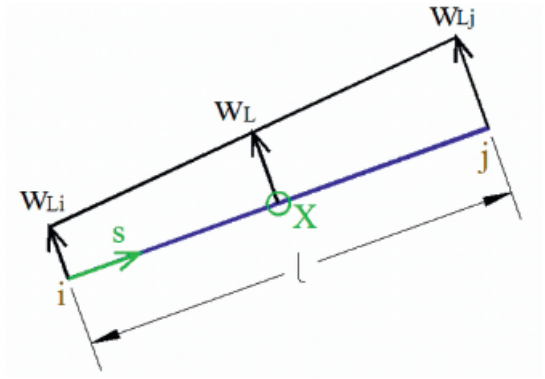

Figure 5.
Deflections perpendicular to the plate plane

Eqs (42) and (43) are rewritten to the form:

$$\begin{bmatrix} w_{Li} \\ w_{Lj} \end{bmatrix} = \begin{bmatrix} t_z & -t_y & 0 & 0 \\ 0 & 0 & t_z & -t_y \end{bmatrix} \begin{bmatrix} u_{yi} \\ u_{zi} \\ u_{yj} \\ u_{zj} \end{bmatrix} \tag{44}$$

Matrix built up from the direction vector $\hat{\mathbf{t}}$ components is called matrix $\mathbf{T}_{\mathrm{L}}$.

The relation between nodes i and j is as follows (in form of $w_L = \mathbf{N}_s \mathbf{v}_{Lw}$):

$$w_{\mathrm{L}}(s) = \left[\left(1 - \frac{s}{l}\right) \frac{s}{l} \right] \begin{bmatrix} w_{Li} \\ w_{Lj} \end{bmatrix} \tag{45}$$

where interpolation matrix $\mathbf{N}_s$ takes the form:

$$\mathbf{N}_s = \left[\left(1 - \frac{s}{l}\right) \frac{s}{l} \right] \tag{46}$$

Integration through the wall length l is made:

$$\delta\mathbf{v}_{Lw}{}^{\mathrm{T}} \int_{0}^{l} \mathbf{N}_s^{\mathrm{T}} n_x \mathbf{N}_s \, ds \mathbf{v}_{Lw} \tag{47}$$

where n_x is in-plane force equal in this case to the constant in-pane load per unit length of the wall.

From Eqn (47) matrix $\mathbf{N}_{sLx}$ is introduced:

$$\mathbf{N}_{sLx} = \mathbf{T}_{\mathrm{L}}^{\mathrm{T}} \int_{0}^{l} \mathbf{N}_s^{\mathrm{T}} n_x \mathbf{N}_s \, ds \mathbf{T}_{\mathrm{L}} \tag{48}$$

Now, the wall's in-plane deflections are considered (see Fig. 6).

On the cross-section level, nodal deflections w_{ci} and w_{cj}, direction vector $\mathbf{t}$ are defined below:

$$\begin{aligned} w_{ci} &= (u_{yi}, u_{zi}) \cdot \mathbf{t} \\ w_{cj} &= (u_{yj}, u_{zj}) \cdot \mathbf{t} \\ \mathbf{t} &= (t_y, t_z) \end{aligned} \tag{49}$$

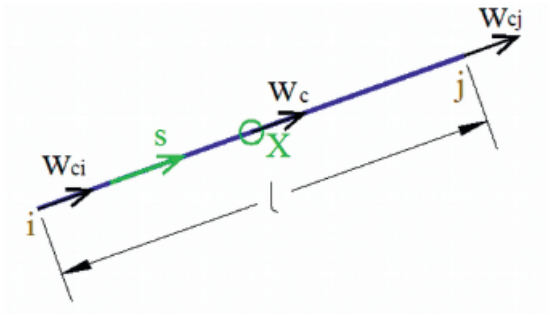

Figure 6.
In-plane deflections

Eqn (49) is rewritten to the form:

$$\begin{bmatrix} w_{ci} \\ w_{cj} \end{bmatrix} = \begin{bmatrix} t_y & t_z & 0 & 0 \\ 0 & 0 & t_y & t_z \end{bmatrix} \begin{bmatrix} u_{yi} \\ u_{zi} \\ u_{yj} \\ u_{zj} \end{bmatrix} \tag{50}$$

and matrix $\mathbf{T}_c$ built up from direction vector $\mathbf{t}$ is introduced.

Using the same procedure presented through Eqs (45)÷(48), matrix $\mathbf{N}_{scx}$ is introduced:

$$\mathbf{N}_{scx} = \mathbf{T}_c^T \int_0^l \mathbf{N}_s^T n_x \mathbf{N}_s \, ds \mathbf{T}_c \tag{51}$$

As the next step, transformation of the interpolation matrix $\mathbf{N}(x)$ achieved in Eqn (35) is presented. From Eqs (4) and (5) the following relations are obtained:

$$\begin{aligned} \mathbf{V}^{bi} &= \mathbf{N}^{v^{bi}} \mathbf{v} \\ \mathbf{V}^{bd} &= \mathbf{T}_{vdi}^b \mathbf{N}^{v^{bi}} \mathbf{v} \end{aligned} \tag{52}$$

and:

$$\begin{aligned} \mathbf{V}^b = \begin{bmatrix} \mathbf{V}^{bd} \\ \mathbf{V}^{bi} \end{bmatrix} = \begin{bmatrix} \mathbf{T}_{vdi}^b \mathbf{N}^{v^{bi}} \mathbf{v} \\ \mathbf{V}^{bi} \end{bmatrix} = \begin{bmatrix} \mathbf{T}_{vdi}^b \\ \mathbf{I} \end{bmatrix} \mathbf{N}^{v^{bi}} \mathbf{v} \\ = \mathbf{T}_{vi}^b \mathbf{N}^{v^{bi}} \mathbf{v} \equiv \mathbf{N}_b \mathbf{v} \end{aligned} \tag{53}$$

where the last equal sign defines interpolation matrix $\mathbf{N}_b$.

Choosing the right rows of $\mathbf{N}_b$ which are related to wall DOF, gives the relation between the wall's DOF vector $\mathbf{v}_b$ and element's DOF vector $\mathbf{v}$.

$$\mathbf{v}_b = \mathbf{N}_b^{v_b} \mathbf{v} \tag{54}$$

For this particular case the external virtual work of TWB element is given as:

$$\delta W^e = \delta \mathbf{v}^T \sum_{walls} \int_0^L \mathbf{N}_{b,x}^{v_b\,T} (\mathbf{N}_{sLx} + \mathbf{N}_{scx}) \mathbf{N}_{b,x}^{v_b} \, dx \, \mathbf{v} \tag{55}$$

From Eqn (55) the element geometry matrix is achieved:

$$\mathbf{k_g} = \sum_{walls} \int_0^L \mathbf{N}_{b,x}^{v_b\,T} (\mathbf{N}_{sLx} + \mathbf{N}_{scx}) \mathbf{N}_{b,x}^{v_b} \, dx \tag{56}$$

For TWB which consists of several elements in x direction, the system geometry matrix is denoted by $\mathbf{K}_g$.

3.2. Eigenvalue solution

After the element stiffness matrix and the element geometry matrix are achieved, an eigenvalue computation is allowed. The virtual work equation for one element is as follows:

$$\delta W = \delta \mathbf{v}^T (\mathbf{k_{el}} + \lambda \mathbf{k_g}) \mathbf{v} \tag{57}$$

From Eqn (57) the finite element equations for the system are of the form:

$$(\mathbf{K} + \lambda \mathbf{K_g}) \mathbf{V} = 0 \tag{58}$$

where $\mathbf{V}$ is the system DOF vector.

4. NUMERICAL PERFORMANCE

The theory described in previous chapters is implemented in *MatLab* [14] and program called "Thin-walled beam statics and stability" (*TWBSaS*) has been created [2]. To check the solutions obtained from *TWBSaS* series of tests were performed. Some of those tests are described in the next subchapters.

4.1. Warping mode

Let's consider an exponential solution to the homogeneous differential equations presented in section 2.2. As an example, symmetric I-profile cross-section is taken with data as follows: E=200 GPa, υ=0.3, t=0.01 m (constant thickness for all walls), G=77 GPa, A=0.05 m^2, Af=0.04 m^2 (flanges area), I=0.0133 m^4 (moment of inertia about strong axis), l=1 m.

One of the exponential modes eigenvalue should correspond to the parameter k described in [6]. Squared value of k is equal to the ratio between the St. Venant torsion stiffness and the warping stiffness and for the I-profile is defined as:

$$k^2 = \frac{GI_t}{EI_w} = \frac{G\frac{1}{3}(2(2l)t^3 + lt^3)}{E\frac{1}{24}l^2(2l)^3 t} \qquad (59)$$

where I_t is the St. Venant torsion stiffness parameter and I_w is the warping stiffness. Using cross-section data and solving Eqn (59) gives constant k equal to 0.013874. This corresponds to exponential mode achieved from TWBSaS, where absolute eigenvalue is equal to 0.013867 (see Fig. 7).

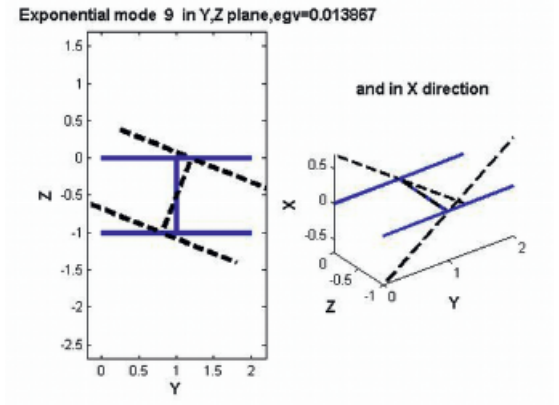

Figure 7.
Cross-section warping

4.2. Column buckling modes

Two examples of cantilever beams subjected to the constant compression load n_x=1GN/m are considered (see Fig. 8). The cross-section data are the same as in previous section.

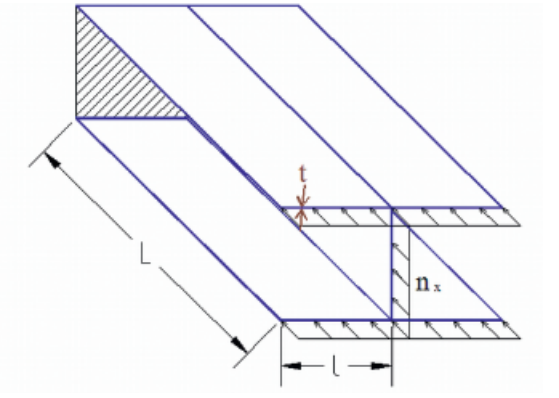

Figure 8.
Cantilever I-column subjected to the constant compression load

Firstly, column buckling mode without shear consideration is investigated. Based on [7], to avoid the effect of shearing force on critical load, the shear deformation parameter Φ has to be much smaller than 1. In this case, to minimize the shear effect, length of the cantilever beam is set up to 5m. This gives value of Φ equal to 0.33 and formula for Euler critical load can be used for comparison. From *TWBSaS*, eigenvalue which corresponds to the column buckling mode is presented in Fig. 9. From Table 1 it can be observed that values achieved from both theories are comparable.

Table 1.
Critical loads for the cantilever I-column without shear consideration

	Eigenvalue (λ)	Critical load [GN]
TWBSaS	0. 478	0.239
Euler formula	-	0.263

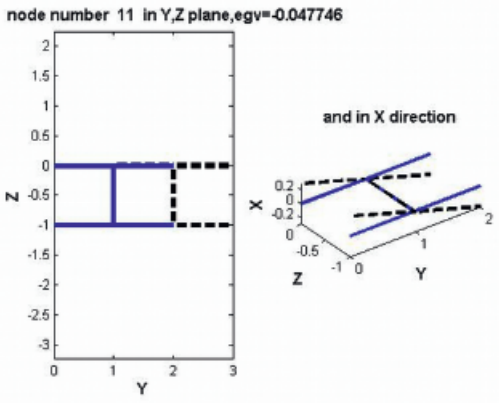

Figure 9.
Column buckling mode without shear consideration

Secondly, column buckling mode with shear consideration is investigated. The same beam's cross-section data and the boundary condition are used as in previous example. This time the effect of shearing force on critical load is taken into account and because of that the shear deformation parameter Φ should have the value around 1. To fulfil this restriction, the value of L=2.5 m with Φ=1.33 is considered. Based on theory described in [11], the formula for a critical load which takes the effect of shearing force into account is given as follows:

$$P_{T1} = \frac{P_E}{1 + nP_E/AG} \qquad (60)$$

where numerical factor n for I-profile is defined as the ratio between area of the I-profile to the area of two flanges multiplied by 1.2.

From *TWBSaS*, eigenvalue which corresponds to the column buckling mode with shear consideration is presented in Fig. 10. From Table 2 it can be observed that values achieved from both theories are comparable.

Table 2.
Critical loads for the cantilever I-column with shear consideration

	Eigenvalue (λ)	Critical load [GN]
TWBSaS	0. 1495	0.748
P_{T1} (Eqn. 60)	-	0.745

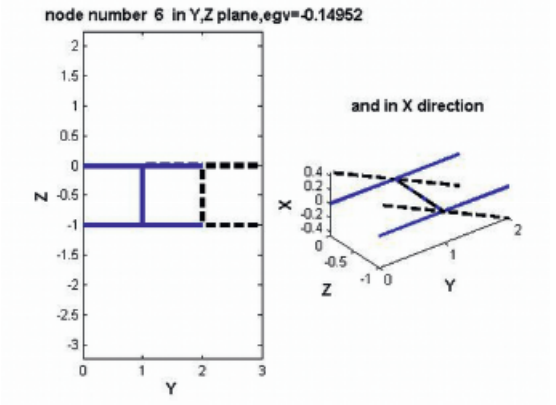

Figure 10.
Column buckling mode with shear consideration

4.3. Torsional buckling mode

Torsion buckling mode is found for a cruciform column which is fixed at the one end and free at the other. The column is subjected to constant compression load n_x=1 GN/m (see Fig. 11).

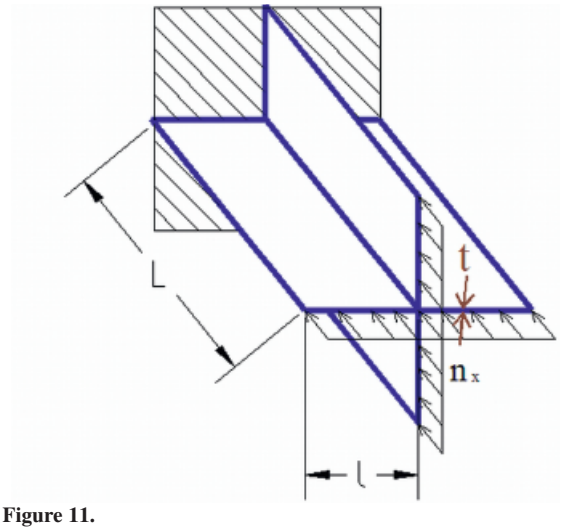

Figure 11.
Cantilever cruciform column subjected to the constant compression load

The cross-section is taken with data as follows: E=200 GPa, υ=0.3, t=0.01 m (constant thickness for all walls), G=77 GPa, A=0.01 m^2, I=1.04*10^{-4} m^4 (moment of inertia), I_p=2.08*10^{-4} m^4 (polar moment of inertia), I_t=3.3*10^{-7} m^4, l=0.25 m. The critical load for uncoupled torsion instability of end-loaded column is calculated using theory presented in [6]. This critical load is given by means of the below formula:

$$P_\varphi = \frac{A}{I_p}[GI_t + \frac{\pi^2 EI_w}{L_{ef}^2}] \tag{61}$$

For the cruciform cross-section, warping rigidity (I_w) is neglected and because of that the critical buckling load is independent of the length of the column. Using Eqn (61), the critical load for torsion buckling is equal to 0.00122 GN. From TWBSaS, eigenvalue which corresponds to torsional buckling mode is presented in Fig.12. From Table 3 it can be observed that values achieved from both theories are the same.

Table 3.
Critical loads for the torsional buckling

	Eigenvalue (λ)	Critical load [GN]
TWBSaS	0.00123	0.00123
Pφ (Eqn. 61)	-	0.00122

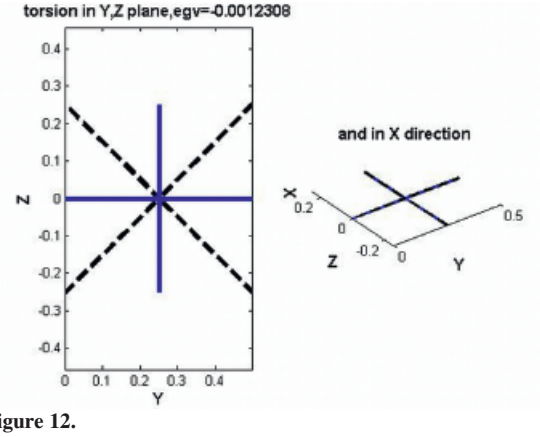

Figure 12.
Torsion buckling mode

4.4. Global, distortional and local buckling modes

In this section basic analysis of the simply supported TWB with hollow-core rectangular cross-section where only compression load in x-direction (n_x=1 GN/m) is considered (see Fig. 13).

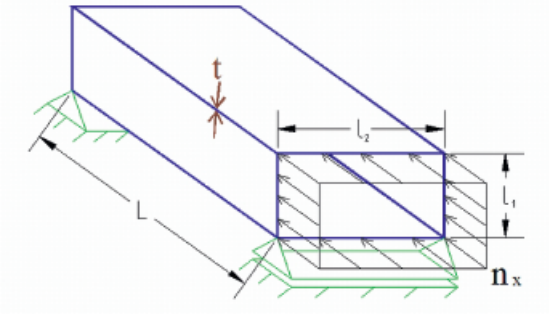

Figure 13.
Simply supported hollow-core beam subjected to the constant compression load

The cross-section has data as follows: E=200 GPa, υ=0.3, t=0.01m (constant thickness for all walls), G=77 GPa, A=0.03 m^2, $I_y=1.46*10^{-3}$ m^4, $I_z=4.17*10^{-3}$ m^4, $l_1=0.5$ m (length of the vertical wall), $l_2=1$ m (length of the horizontal wall). The total length of the beam is equal 3 m.

The stability modes achieved so far in the previous examples are for cases where buckling modes involve only modes with long waves in x-direction (global column buckling modes). So in this section, we will mostly focus on distortional and local plate buckling modes. For local plate buckling modes several short waves between two ends of the TWB are involved. The example of distortional buckling mode with eigenvalue λ=-0.116 is presented in Fig. 14. It seems that critical load 0.348 GN (λ=-0.116) is reasonable because it is slightly bigger than critical load achieved from column buckling about weak axis which is equal to 0.312 GN (λ=-0.104). It is due to bending stiffness consideration in the cross-section of each wall. Both values are achieved from *TWBSaS*.

The stability mode which satisfies the classical local plate buckling mode for the eigenvalue λ=-0.000506 is found by *TWBSaS* (see Fig. 15). This eigenvalue corresponds to critical load $n_{cr}=0.000506$ GN/m. This mode consists of 5 half-waves in longitudinal direction.

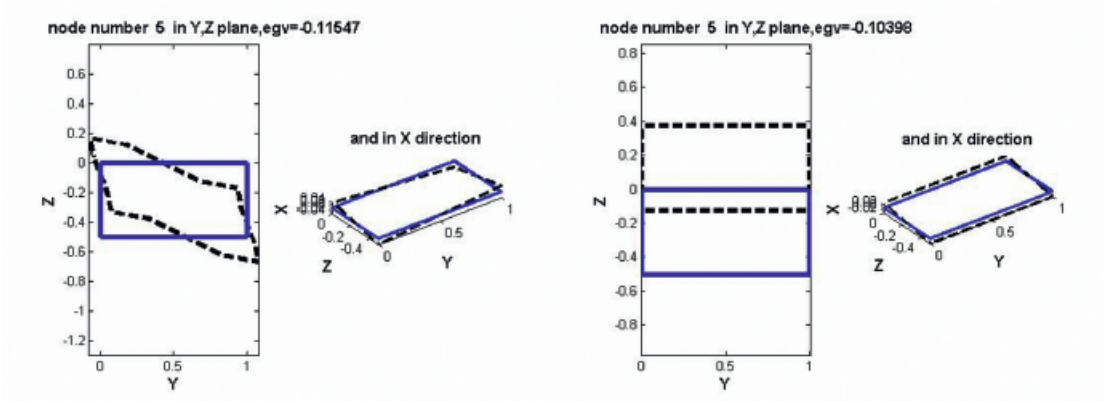

Figure 14.
Distortional and global column buckling modes

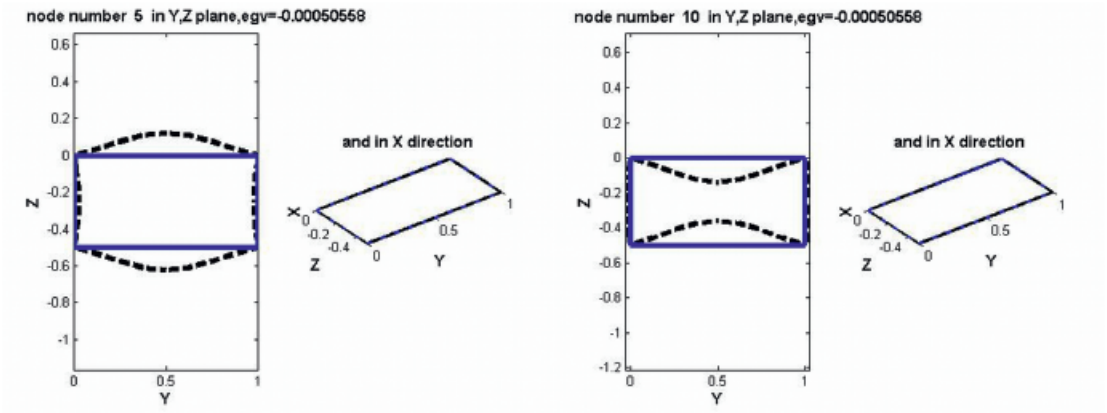

Figure 15.
Local plate buckling mode

Using the plate buckling theory presented in [8], critical stability load can be calculated and compared with one achieved from *TWBSaS*. To do this, only one wall of the TWB cross-section (upper horizontal wall) as simply supported rectangular plate is considered. The deflection field in the plate is chosen as follows:

$$w(x,y) = c\sin\frac{m\pi x}{L}\sin\frac{n\pi y}{l_2} \tag{62}$$

where c is an arbitrary constant and m=3 and n=1 give the number of half-waves in x and y direction respectively. Based on [8] the critical buckling load is determined by:

$$n_x = k\frac{\pi^2 D}{(l_2)^2} \tag{63}$$

where D is the plate bending stiffness and stability coefficient k is as follows:

$$k = \left(\frac{ml_2}{L} + \frac{L}{ml_2}\right)^2 \tag{64}$$

Eqn (64) gives k=4, D=1.8*10^{-5} GNm and substituting this values to Eqn (63) gives the plate critical buckling load equal to 0.000723 GN/m.

It is observed that value achieved from Eqn (63) and values form *TWBSaS* differ from each other. The fact of different amount of half-waves in x-direction is taken into account. It seems that local plate buckling theory is not fully included in the present work. The theory presented in previous chapters does not include term for bending stiffness perpendicular to the plate plane in longitudinal direction. It means that critical load concerning the local plate buckling achieved form TWBSaS is smaller than the one from Eqn (63). It is also observed that by mesh increase in the elements (cross-section walls and longitudinal elements) the results given by means of the program are getting more accurate but do not fully coincide with the well known plate theory. So critical loads for local plate buckling achieved from *TWBSaS* can be inaccurate and further investigation is needed.

5. CONCLUSIONS AND FUTURE WORK

During this research work statics and stability of the thin-walled shear beam with cross-section distortion were studied. Next, the program based on that theory has been written in *MatLab* [14] and called *TWBSaS* [2]. This program is based on the well known beams theories and does not involve large amount of degrees of freedom. Results given by that program are checked with existing theories and the following was observed:

- based on [6], eigenvalue which corresponds to the warping mode for I-profile cross-section is calculated. This value is very similar to the one achieved from TWBSaS. It can be stated that exponential solution gives the reasonable values of eigenvalues.
- based on Euler load calculation, the critical column buckling load was found and compared with the one given in *TWBSaS*. Both solutions are similar.
- based on [11], the critical column buckling load with shear consideration was calculated and compared with the one achieved from *TWBSaS*. Both solutions are similar.
- based on [6], the critical torsion buckling mode is calculated and compared with the one given in *TWBSaS*. Both solutions are very similar.
- based on [8], the local plate critical buckling was calculated and compared with the one given in *TWBSaS*. Both results differ from each other due to the lack of the term for bending stiffness perpendicular to the plate plane in longitudinal direction. The further investigation of local plate buckling theory is necessary.

As for the future work, except local plate buckling theory investigation, the program should be checked for cases with more complicated load cases e.g. in-plane banding, in-plane non-uniformly distributed load. Furthermore, research about dynamics of TWB with cross-section distortion would be important issue to consider from the engineering point of view. The theory presented in this paper can be a useful tool to investigate stability problems of ABM K-span steel buildings, where for European Standards (according to authors) non research has been done [12].

ACKNOWLEDGEMENTS

We would like to show our gratitude to Associate Prof. Leif Otto Nielsen and Prof. Jeppe Jönsson from Department of Civil Engineering at the Technical University of Denmark where the research used for this publication has been done.

REFERENCES

[1] *Adany S., Schafer W.*; Understanding and classifying local, distortional and global buckling in open thin-walled members. Annual Conference, Structural Stability Research Council, Montreal, Canada, 2005

[2] *Cybulski R.*; Statics and stability for thin walled shear beam with cross-section distortion. Technical University of Denmark, Department of Civil Engineering, 2010

[3] *Cybulski R.*; Numerical issues on beam finite elements. Report Master MEMS-GGCR, Laboratoire Sols, Solides, Structures- Risques, INP/UJF/CNRS, 2008

[4] *Grabiec K.*; Konstrukcje Cienkościenne (Thin-walled structures). Państwowe Wydawnictwo Naukowe, Warszawa-Poznań, 1976 (in Polish)

[5] *Jonsson J.*; Distortional theory of thin walled beams. Thin-Walled Structures, Vol.33, 1999, p.269-303

[6] *Krenk S.*; Lectures on thin-walled beams. Technical University of Denmark, Department of Mechanical Engineering, January 2006

[7] *Krenk S.*; Mechanics and analysis of beams, columns and cables. 2nd ed. Springer-Verlag, Berlin, Heidelberg, New York, 2001

[8] *Nielsen L.O.*; Elements of plate bending statics. Technical University of Denmark, Department of Civil Engineering, 2008

[9] *Nielsen L.O.*; Finite element methods for structural engineering. Technical University of Denmark, Department of Civil Engineering, 2008

[10] *Nielsen L.O.*; Thin-walled beam statics with cross-section distortion. Technical University of Denmark, Department of Civil Engineering, 2009

[11] *Timoshenko S.P., Gere J.M.*; Theory of elastic stability. McGraw-Hill Book Company Inc., 1961

[12] *Walentyński R.*; Design problems of cold formed lightweight ark structures. Lightweight structures in civil engineering, Local seminar of IASS Polish Chapter, Warsaw-Czestochowa, 2004

[13] *Vlasov V.Z.*; Thin-walled elastic beams. 2nd ed. Israel Program for Scientific Translations, Jerusalem, Israel, 1961

[14] MatLab; http://www.mathworks.com